Journal of Sound and Vibration (1978) **56**(1), 105–125

AN EFFICIENT METHOD OF MEASURING IMPEDANCES OF FLUID MACHINERY MANIFOLDS

R. SINGH† AND W. SOEDEL

Ray W. Herrick Laboratories, School of Mechanical Engineering, Purdue University, West Lafayette, Indiana 47907, *U.S.A.*

(*Received* 10 *December* 1976, *and in revised form* 3 *September* 1977)

Knowledge of the acoustical impedances is required to understand the fluid oscillations in the manifolds of positive displacement machinery. This paper presents an impedance measurement method which puts emphasis on the lower frequencies. The technique is based on providing a known volume velocity excitation to the manifold through an electrodynamic, shaker driven, oscillating piston. Harmonic, random and transient excitations have been utilized. Digital data acquisition and processing techniques are used to acquire piston displacement and acoustic pressure signals for input and transfer impedances. The proposed method is direct and efficient. It is applied to the measurement of the acoustical impedances of a two-cylinder refrigeration compressor discharge system. Various aspects of the measurement procedures are discussed along with the recommendations.

1. INTRODUCTION

The nature of fluid oscillations in the manifolds of positive displacement machines (internal combustion engines, compressors and pumps, etc.) often needs to be assessed for design and evaluation purposes. Manifold fluid pressure oscillations interact with the cylinder (i.e., source) processes. This can be termed the back pressure effect. Generally the lower frequency pulsations affect performance and energy requirements. Pulsations can also be responsible for noise and vibration problems of positive displacement machines, interconnected pipes and other attached components.

Acoustical theory, in which an approximately linear relationship is assumed between pressure and density changes about an operating point (mean pressure and mean density), is widely utilized to analyze these flows, as long as pressure amplitudes are less than about 20% of the ambient pressure. The emphasis has mostly been on the control and suppression of flow oscillations through the use of mufflers or flow smoothing devices. But, no matter how close the muffler is attached to the cylinder, one still finds some components in between it and the valves. Also, the pulsations are still dominant in these components as mufflers are generally of the reactive type, which attenuate fluid-borne noise by reflecting back sound waves towards the source: i.e., cylinder. Furthermore, in a large number of situations, multicylinder machines are encountered. Their manifolds are generally designed to either distribute or collect fluid flows. A complicated oscillatory behavior is produced in these manifolds because of the dynamic interactions between cylinders. Both constructive and destructive acoustic interference can be observed.

If the interest is mainly in the evaluation of the effectiveness of a muffler, then knowledge of only the muffler transmission characteristics is adequate. But for the study of the overall dynamic nature of the manifolds, both magnitude and phase of complex acoustical characteristics of the muffler and the manifold are required. The muffler can be considered to be

† Currently with Carlyle Compressor Company, Carrier Corporation, Syracuse, New York 13201, U.S.A.

part of the manifold. The characteristics that have to be known are the acoustical impedances. They define the dynamic nature of the manifold. They can be incorporated in a mathematical simulation model, together with source and termination information.

The purpose of measuring manifold acoustical impedances could be any one or a combination of the following: (a) to determine resonant frequencies and model parameters of fluid oscillations, (b) to gain an understanding of the wave interference mechanism in the multicylinder manifolds, and (c) to build mathematical models for the purpose of predicting pressure oscillations. In fact, the authors have been successful in utilizing impedances for the simulation of dynamic processes in a multicylinder compressor [1, 2]. In this study, the discharge system is described by steady state acoustical impedances, and these are coupled with the time variant cylinder and valve models. An iterative procedure is utilized to account for the back pressure effect. Although only theoretically computed impedances have been utilized, one can very well use measured acoustic impedances as input in the computer simulation program. This is attractive when one is faced with practical manifolds whose mathematical formulation would prove to be too complicated and time consuming. Also, for certain components, especially those exhibiting non-linear effects, one may not be able to describe them with the existing theory. Under such conditions, measured average impedances could be utilized to build mathematical models. Furthermore, measured impedances can always be used to verify the theoretical computations.

2. MEASUREMENT OBJECTIVES AND LITERATURE REVIEW

The aim of the investigation reported here was to develop a method for measuring both input and transfer acoustical impedances. The frequency range of interest has the following limits.

1. *Lower frequency limit.* The major emphasis of the experimental program is on the lower frequencies, as the first few harmonics of the running speed of a positive displacement machine are important from the machine performance viewpoint. For example, consider the case of a high speed refrigeration compressor. The operating speed is of the order of 3600 rev/min, and thus the measurement of system dynamic characteristics at the first harmonic, i.e., 60 Hz, is essential.
2. *Upper frequency limit.* The investigation is focused only on the plane wave frequency region because of the following reasons: (a) generally lower frequency pulsations are dominant, (b) transverse dimensions of manifolds are often smaller than the shortest wave length of interest, (c) plane wave mathematical formulations of manifolds have been found to be adequate for simulation purposes [1, 2], and (d) the acoustic pressure can be measured easily and reliably in the plane wave region. Thus the study is limited to measurement applications for "acoustically small" positive displacement machinery manifolds.

Gatley and Cohen [3, 4] reviewed the previous experimental methods and concluded that only a few investigators directed their attention to the evaluation of small acoustic filters. For such a system, they recommended an evaluation procedure which employs a standing wave tube of "unique design". Perhaps the standing wave tube method is the most attractive method as it does not require absolute measurements. It has been used by a large number of investigators [5–9], but they have mostly concentrated on the performance evaluation of mufflers and absorption materials. In these investigations attempts have not been made to measure lower frequency characteristics because of the inherent lower frequency limitation of the standing wave tube method [6]. For example, the required length of the microphone traverse would be about 20 feet for measurements at 50 Hz in air. This poses measurement reliability problems. Furthermore, a precise measurement of impedance requires an exact

location of the minima. Slight error in the position could result in large variation of the acoustical impedances. The standing wave tube method is very time-consuming as only one frequency measurement can be conducted at a time. Also, only the input impedance is measured. However, for the present study, a preliminary investigation was carried out with Gatley's standing wave tube [4]. Since the diameter of the unknown impedance termination was about 1·5 inches, Gatley's tube of 1·5 inch I.D. was chosen. According to ASTM standards [6], the upper frequency limit was 5 kHz and the lower frequency limit was 600 Hz. Although one maximum and minimum were obtained down to 300 Hz, two successive minima are required for the measurement of impedances. These were obtained at 700 Hz and higher frequencies.

The two-pressure method has been used for the impedance measurement of resonant expansion chambers and porous materials [8]. It is useful only when the impedance at one point is known. A three-pressure method has also been tried for determining reflection factors of muffler elements [3]. But the method is unreliable from an accuracy viewpoint.

The pulse or transient method employs a "tone-burst" sound pulse [3, 4, 9]. It is reported that it requires long lengths of tubing because the reflected wave from an unknown impedance termination should arrive only after the incident wave signal. Such long tubes cause severe attenuation of the waves. Also, filters with rapid transient response are required. The pulse transient method is basically a single frequency measurement.

Measurement of four-pole coefficients has been tried to determine the absorption and attenuation characteristics [10, 11]. Furthermore, according to Salara [12], the use of acoustic and electro-acoustic bridges is time-consuming and usually gives no guarantee to furnish as accurate a measurement as their electric counterparts give in the audio frequency range. Salara [12] has also constructed acoustical sources of the constant volume velocity type.

An overall survey of all of the available methods has revealed the following.

1. All methods seem limited as they are not practical for large wavelengths, which means low frequencies.
2. Sound excitation sources, particularly horn drivers, have a lower frequency limitation. Generally it is about 100–200 Hz. Thus, when using a horn driver, harmonic excitation cannot be simulated for the first few harmonics of a typical positive displacement machine.
3. It is difficult to measure particle or volume velocity directly. The state of the art is such that measurements of particle or volume oscillation velocity for the purpose of impedance determination are not performed in practical applications.
4. Methods generally do not allow for a direct measurement of both input and transfer impedances.

3. PROPOSED METHOD: KNOWN VOLUME VELOCITY EXCITATION TECHNIQUE

The impedance measurement at a particular point requires the measurement of both pressure and volume velocity. As the volume velocity at any arbitrary point cannot be measured, a known volume velocity signal can be fed to the system. For this, a sound source is needed which not only provides the excitation but also whose velocity signal can be monitored. A horn driver could be used for this purpose. The displacement of the horn driver could probably be measured in any one of the following ways: (i) monitor pressure in the small cavity, behind the diaphragm, with a microphone and then relate it to the displacement, (ii) monitor displacement with a displacement transducer, and (iii) mount a non-driven horn driver in between the exciter and the system and use it as a transducer. Unfortunately,

the lower cut-off frequencies of horn drivers rule out the possibility of low frequency excitations.

The solution was to use a harmonically oscillating piston as driver. The reciprocating action of the driver piston is equivalent to a change in volume at the piston location which

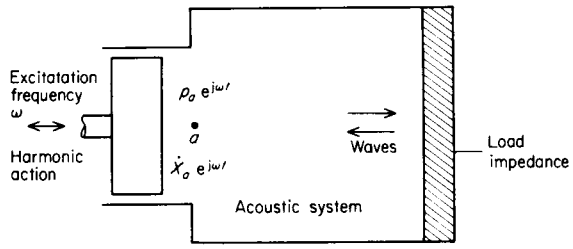

Figure 1. Harmonically oscillating piston as an input to the acoustic system.

causes a change in density and thus in pressure. These changes are transmitted as waves with the speed of sound into the manifold, become reflected and form a pressure and particle velocity pattern that is characteristic of the system. The resulting pressures and velocities are both time and spatial dependent. The piston motion can be considered as an input to the

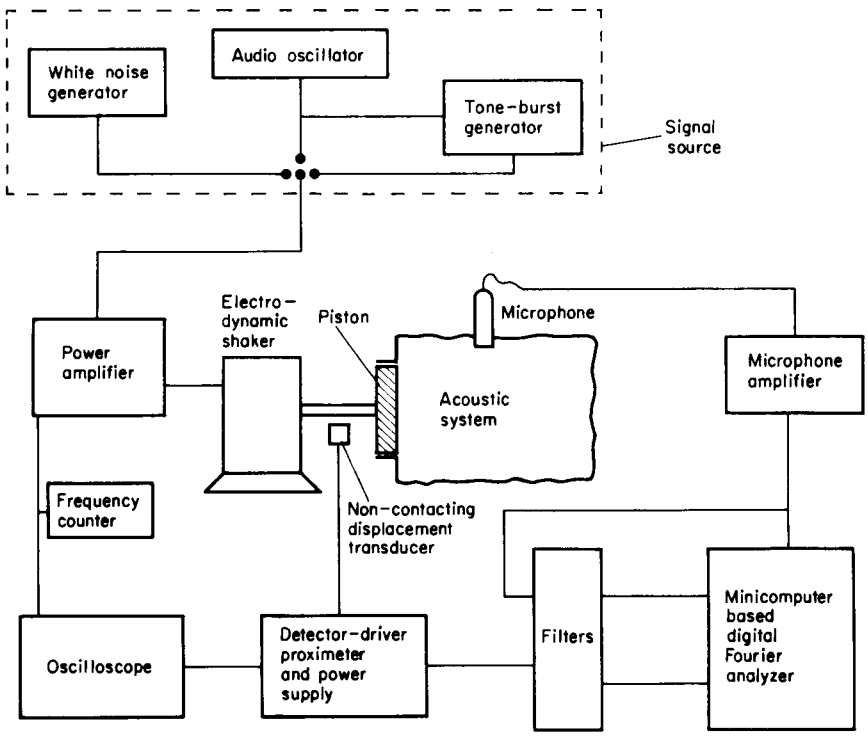

Figure 2. Schematic of instrumentation for impedance measurement.

acoustic system. Since the reciprocating action is nothing but simple harmonic motion, the piston motion can be considered as the forced harmonic velocity input to the system. As the acoustic system is dynamically linear in nature, its response will be only at the driving frequency corresponding to that of the reciprocating motion. This is illustrated in Figure 1. If the displacement of the piston is monitored, then the input volume velocity is known. The pressures can be measured by using microphones.

Instrumentation for the proposed method can be grouped into excitation, volume velocity measurement, and pressure measurements. A schematic of the instrumentation is presented in Figure 2.

1. *Excitation.* The piston can be driven by an electrodynamic shaker. The piston is mounted on the moving element of the shaker. For the harmonic method, the shaker was driven by an audio oscillator and amplifier. The frequency of excitation was monitored by a frequency counter. The dynamic characteristics of the electrodynamic shaker were as follows: rated force 25 lbf (112 N); frequency range 5 Hz–15 kHz, bare table; axial resonant frequency 15 kHz, bare table; maximum bare table acceleration 71 g (700 m/s^2); maximum displacement amplitude 0·25 in (6·35 mm); maximum velocity 98 in/s (2·5 m/s) peak; dynamic weight of the moving element 0·35 lb (160 g). With introduction of an 0·25 lb piston and fastening rod, the axial resonant frequency was lowered to 14·5 kHz. For the transient and random methods, the frequency response can be adjusted by a control circuit to be constant throughout the band of frequencies used in the measurements. However, a flat frequency response is not a requirement in any of the methods since the input, namely the piston velocity, is measured directly and analyzed directly, together with the measured response pressures.
2. *Volume velocity measurement.* The volume velocity at the piston can be calculated from the piston displacement. It is monitored by a non-contacting displacement transducer. A detector driven proximeter and power supply are used in conjunction with the transducer. The displacement signal can be displayed on an oscilloscope. It can be analyzed along with the pressure signal by a frequency analyzer. The calibration of the displacement transducer signal was done by providing the piston with known static displacements.
3. *Pressure measurement.* The pressure in the acoustic system, at any location, can be monitored by a microphone. For the present work 1/4 inch microphones were flush mounted in the system. The microphone signal can be amplified and then sent to the analyzer. A minicomputer based digital Fourier analyzer with Fast Fourier Transform capability was utilized for data acquisition and processing. Both displacement and pressure signals are acquired simultaneously after the triggering provided by the displacement signal.

4. MEASUREMENT PROCEDURES

4.1. HARMONICALLY OSCILLATING PISTON METHOD

The piston method, as proposed in the last section, allows acoustical impedances to be calculated directly as per the definition, which is that the impedance is the complex quotient of pressure and volume velocity.

An audio oscillator provides the harmonic signal (see Figure 2) to the electrodynamic shaker. The piston, in turn, executes a harmonic motion which is monitored by a displacement transducer. The acoustic medium experiences steady state harmonic oscillations, whose pressure is monitored by a microphone. Both displacement and pressure signals are multiplied by calibrated scale factors to obtain the displacement, $x(t)$, and pressure, $p(t)$ (a list of symbols is given in the Appendix). In the time domain, the signals look as shown in Figure 3. The time period corresponds to the excitation frequency ω_e as set on the audio oscillator. As the impedance is defined in the frequency domain, the discrete Fourier transform technique is used to convert the signals to the frequency domain [13]:

$$x(\omega) = \int_{-\infty}^{\infty} x(t)\, e^{-j2\pi ft}\, dt, \tag{1}$$

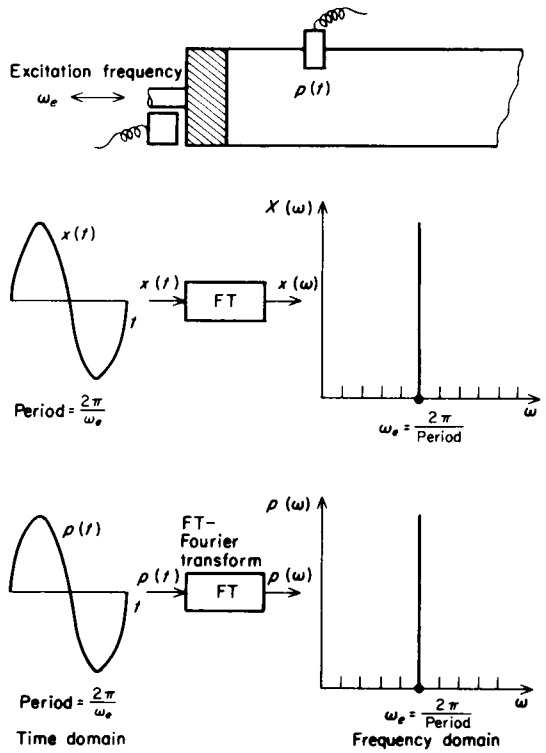

Figure 3. Displacement and pressure signals for harmonic excitation.

or, in terms of samples,

$$x(\omega) = x(m\Delta f) = \Delta t \sum_{n=0}^{N-1} x(n\Delta t)\, e^{-j2\pi(m\Delta f)(n\Delta t)}, \tag{2}$$

where N is the total number of samples, Δf and Δt are frequency and time resolutions, respectively, $n(n = 0, 1, \ldots, N-1)$ is the sample number in the time domain and $m(m = 0, 1, \ldots, \frac{1}{2}N - 1)$ is the sample number in the frequency domain. If T is the time window, $f_{\max}$ is the upper frequency limit of the desired frequency domain, and f_s is the sampling frequency:

$$T = N\Delta t = N/f_s, \qquad f_{\max} = \tfrac{1}{2}N\Delta f = f_s/2, \qquad \Delta f = 1/T. \tag{3–5}$$

Relationships (3)–(5) suggest that only two of the five variables T, N, Δf, f_s or Δt and $f_{\max}$ are required to be set. The same procedure follows for pressure also.

Standard digital data analysis procedures such as sampling considerations, data acquisition operations, filtering, Fast Fourier Transform (FFT) computations and other data processing techniques were applied. A detailed discussion of these is readily available in the literature [13, 14].

In the frequency domain, the pressure ($p(\omega)$) and displacement ($x(\omega)$) spectra have only one dominant component. It is at the excitation frequency ω_e (see Figure 3). At other frequencies, there may be some values but these will be insignificant and minor compared to ω_e. These values belong to noise, either in the instrumentation or from the ambient noise level in the acoustic system, or from perturbations in the harmonic motion of the excitation piston.

The displacement spectra can be changed into volume velocity spectra, $\dot{X}(\omega)$, with the help of the relationships

$$\dot{X}(\omega) = \int_{-\infty}^{\infty} \dot{X}(t)\, e^{-j2\pi ft}\, dt, \tag{6}$$

$$\dot{X}(\omega) = \dot{X}(m\Delta f) = \Delta t \sum_{n=0}^{N-1} \dot{X}(n\Delta t)\, e^{-j2\pi(m\Delta t)\cdot(n\Delta t)}, \tag{7}$$

where

$$\dot{X}(t) = S\, dx(t)/dt, \qquad X(\omega) = S(j\omega)\, x(\omega), \tag{8,9}$$

and where S is the cross-sectional area at the piston. The impedance spectrum $Z(\omega)$ is obtained by dividing the pressure spectrum $p(\omega)$ by the volume velocity spectrum $\dot{X}(\omega)$ [15, 16] (again, the impedance spectra will also have only one major component, corresponding to ω_e; recall that $p(\omega_e)$, $\dot{X}(\omega_e)$ and $Z(\omega_e)$ are all complex quantities; the subscript e stands for excitation frequency):

$$p(\omega_e) = p_R(\omega_e) + j\, p_I(\omega_e) = |p(\omega_e)|\, e^{j\psi_p(\omega_e)}, \tag{10}$$

$$\dot{X}(\omega_e) = \dot{X}_R(\omega_e) + j\dot{X}_I(\omega_e) = |\dot{X}(\omega_e)|\, e^{j\psi_{\dot{X}}(\omega_e)}, \tag{11}$$

$$Z(\omega_e) = \frac{P(\omega_e)}{\dot{X}(\omega_e)} = \frac{P_R(\omega_e) + j\, p_I(\omega_e)}{\dot{X}_R(\omega_e) + j\, \dot{X}_I(\omega_e)} = \left|\frac{p(\omega_e)}{\dot{X}(\omega_e)}\right| e^{j[\psi_p(\omega_e) - \psi_{\dot{X}}(\omega_e)]} \tag{12}$$

$$= |Z(\omega_e)|\, e^{j\psi_Z(\omega_e)} = Z_R(\omega_e) + j\, Z_I(\omega_e). \tag{13}$$

In terms of pressure and displacement signals, $Z(\omega_e)$ is

$$|Z(\omega_e)| = |p(\omega_e)/\dot{X}(\omega_e)|, \qquad \psi_Z(\omega_e) = \psi_p(\omega_e) - \psi_{\dot{X}}(\omega_e) - \pi/2. \tag{14,15}$$

The procedure provides the impedance information at the excitation frequency ω_e. It can be repeated for other desired frequencies. Now only one question remains: how to determine input and transfer impedances? The experimental procedure follows the definitions. With reference to Figure 4, input (Z_{ii}) and transfer (Z_{iq}) impedances are

$$Z_{ii}(\omega) = p_i(\omega)/\dot{X}_i(\omega), \qquad Z_{iq}(\omega) = Z_{qi}(\omega) = p_q(\omega)/\dot{X}_i(\omega). \tag{16,17}$$

As impedance measurements are generally conducted for air at room temperatures, Z_{ii} and Z_{iq} are for air only. To make these results universal, i.e., applicable to all media, at any temperature, the impedances should be presented in dimensionless form:

$$\bar{Z}(\omega_e) = Z(\omega_e)/\rho c/S, \tag{18}$$

where $\bar{Z}(\omega_e)$ is the dimensionless impedance. It should be plotted against either wavelength (λ) or wave number (k). If it is plotted versus frequency (ω), the resonances would correspond

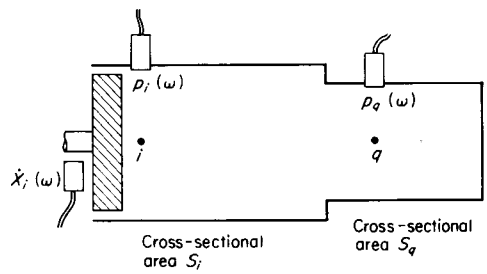

Figure 4. Input and transfer impedance measurement.

to a particular medium only; plotting against k or λ will make it applicable to all media (for the same manifold geometry, of course).

4.2. RANDOMLY OSCILLATING PISTON METHOD

The harmonically oscillating piston method provides only some discrete frequency points. If an impedance needs to be determined at some particular frequency, then the system has to be driven at that frequency only, through an audio oscillator. Thus, for a complete impedance

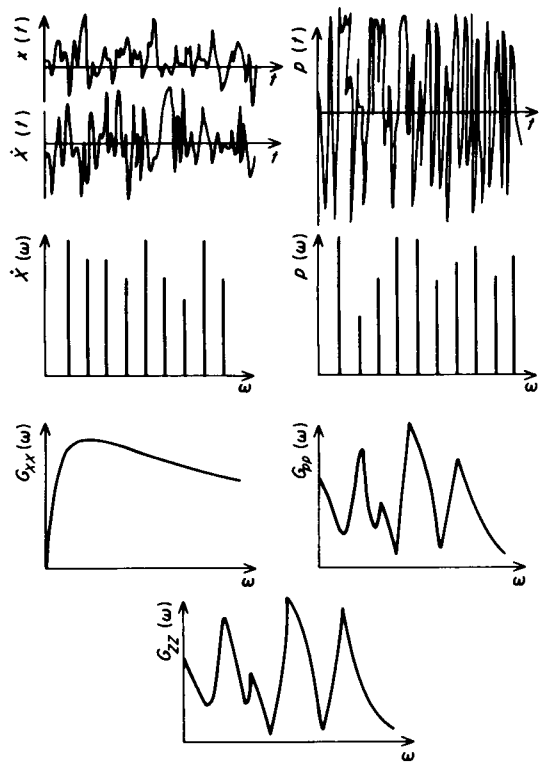

Figure 5. Randomly oscillating piston method.

spectrum, a large number of points are required. Nevertheless, with discrete points there is always the possibility of missing a peak or valley in the spectrum plot. Thus it is essential to obtain a continuous impedance curve. To overcome this drawback, a different excitation is proposed here.

The piston method, as proposed in the previous section, works on the principle of harmonic excitation. Now, if an excitation composed of several frequencies is fed to the acoustic system, then the system response is a steady state oscillation which is composed of all of the excitation frequencies. A periodic non-random signal is a good example of such excitation. But still, it is composed of only some frequencies which are multiples of each other. What is needed is a source which can provide excitation at all frequencies. A random noise source can be considered such an excitation.

The shaker can be driven by a random noise source. For this investigation, a white noise generator was used. As the shaker driven piston moves randomly the pressures monitored by the microphones are random signals (see Figure 5). Both $p(\omega)$ and $\dot{X}(\omega)$ spectra show

signs of all frequencies. The impedance $Z(\omega)$ can be determined from the following relationships:

$$Z(\omega) = G_{p\dot{X}}(\omega)/G_{\dot{X}\dot{X}}(\omega) = |Z(\omega)|\, e^{j\psi_Z(\omega)}, \tag{19}$$

where G signifies the power spectrum,

$$G_{p\dot{X}}(\omega) = p(\omega)\, \dot{X}^*(\omega), \qquad \text{the cross-power spectral density,} \tag{20}$$

$$G_{\dot{X}\dot{X}}(\omega) = \dot{X}(\omega)\, \dot{X}^*(\omega) = |\dot{X}(\omega)|^2, \qquad \text{the auto-power spectral density (volume velocity),} \tag{21}$$

$$G_{pp}(\omega) = p(\omega) p^*(\omega) = |p(\omega)|^2, \qquad \text{the auto-power spectral density (pressure),} \tag{22}$$

and where the symbol * signifies the complex conjugate. The impedance magnitude and phase are, respectively,

$$|Z(\omega)| = |G_{p\dot{X}}(\omega)/G_{\dot{X}\dot{X}}(\omega)| = |p(\omega)\, \dot{X}(\omega)/|\dot{X}(\omega)|^2|, \tag{23}$$

$$\psi_Z(\omega) = \psi_{G_{p\dot{X}}}(\omega) - \psi_{G_{\dot{X}\dot{X}}}(\omega) = \psi_p(\omega) + \psi_{\dot{X}^*}(\omega) - \psi_{\dot{X}}(\omega) - \psi_{\dot{X}^*}(\omega) = \psi_p(\omega) - \psi_{\dot{X}}(\omega). \tag{24}$$

The impedance power spectrum $G_{ZZ}(\omega)$ is

$$G_{ZZ}(\omega) = G_{pp}(\omega)/G_{\dot{X}\dot{X}}(\omega) = p(\omega) p^*(\omega)/\dot{X}(\omega)\, \dot{X}^*(\omega); \tag{25}$$

also

$$G_{ZZ}(\omega) = Z(\omega)\, Z^*(\omega) = |Z(\omega)|^2. \tag{26}$$

As dimensionless impedance information is more desirable, one can write

$$|\bar{Z}(\omega)| = \{1/(\rho c/S)\}\, |Z(\omega)|, \qquad \psi_{\bar{Z}}(\omega) = \psi_Z(\omega), \tag{27, 28}$$

and the dimensionless impedance power spectrum is

$$G_{ZZ}(\omega) = \{1/(\rho c/S)^2\}\, G_{ZZ}(\omega). \tag{29}$$

Now, one question remains: is the output $p(\omega)$ or response $Z(\omega)$ totally due to the input $\dot{X}(\omega)$? For this coherence function analysis can be performed. The coherence function (γ^2) is a measure of the degree of similarity, dependence and correlation between the input and output. It is, in the frequency domain,

$$\gamma^2(\omega) = |G_{p\dot{X}}(\omega)|^2/G_{pp}(\omega)\, G_{\dot{X}\dot{X}}(\omega), \qquad 0 \leqslant \gamma^2(\omega) \leqslant 1; \tag{30}$$

$\gamma^2(\omega) = 0$ indicates that the output is independent of the input and $\gamma^2(\omega) = 1$ that the output is totally dependent on the input.

The flow diagram of the impedance computation procedure is depicted in Figure 6.

As volume velocity is the input, its power spectrum $G_{\dot{X}\dot{X}}(\omega)$ (Figure 5) is similar to that of the source, the white noise generator. Its frequency range is 20 Hz to 20 kHz. As the present investigation focuses on lower frequencies, filters were used to attenuate the upper frequencies.

This method provides a continuous curve for the impedance spectrum. As the input power is almost constant, the pressure power spectrum resembles the impedance spectrum.

4.3. TRANSIENTLY OSCILLATING PISTON METHOD

Theoretically speaking, an excitation with all the frequencies can be obtained by using an impulse signal. Its frequency spectrum is flat. But, in actual situations, it is hard to get a source which provides a truly impulsive excitation. In structural dynamic systems, a hammer is generally used to achieve such an excitation. Acoustically, it is difficult to generate the equivalent. One can argue, "How about hitting the piston with a hammer?" However, as the piston is very small in size and is also blocked on one side by the transducer, there is not enough room for this. The electronics also was not adequate to generate an impulsive input. Thus, attention had to be diverted to other transient signals.

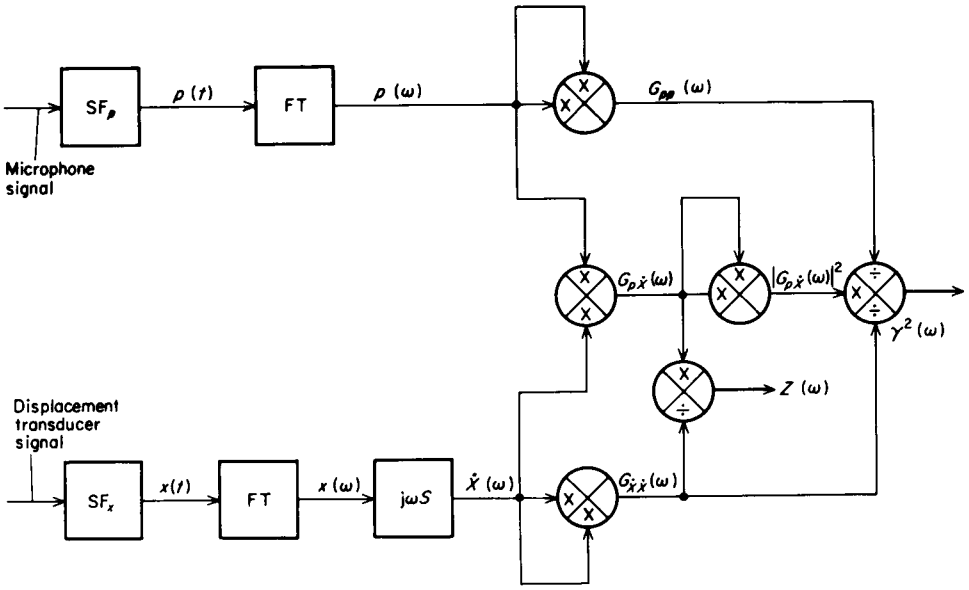

Figure 6. Flow diagram of impedance computation using random and transient excitations. SF, Scale factor; FT, Fourier transform.

A tone-burst generator along with an audio oscillator is used to generate a pulse which is periodic and exists only for a certain fraction of the period. The signal is fed to the shaker and piston. The displacement signal, as shown in Figure 7, is similar to that of the input provided to the shaker. The pressure decays rapidly as the system is experiencing transient oscillations (see Figure 7).

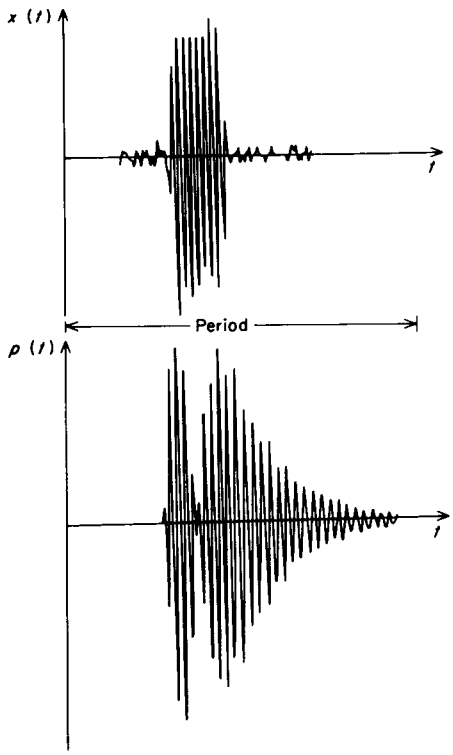

Figure 7. Displacement and pressure signals for transiently oscillating piston method.

The procedure, as illustrated in Figure 6, similar to that of the random excitation, is followed to determine acoustical impedances.

5. MEASUREMENTS AND RESULTS

The example case to which the proposed methods were applied is shown in Figure 8. It is the discharge manifold of a two-cylinder refrigeration compressor. It consists of the following components: discharge plenums (shown as Nos 1 and 2), connecting passages, collector and the muffling system. An anechoic tube is attached to the manifold end, simulating the condensor. An anechoic termination is not a requirement of the methods presente', but is

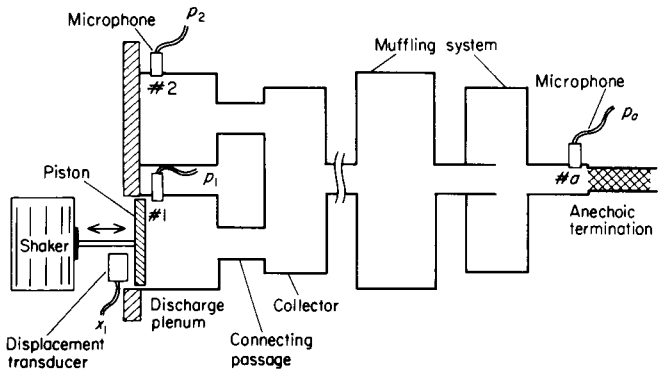

Figure 8. Schematic of the example case, discharge manifold system of a two cylinder compressor.

simply part of the manifold system in this example. It is the standard way in which this refrigeration compressor is evaluated for performance on a test stand. Obviously, one could also separate the manifold system from the anechoic pipe. This would result in different impedance values, to which the anechoic termination could then be added mathematically, or the actual condensor could have been defined as being part of the manifold. The definition of what is and what is not part of the manifold does not affect the methods presented. A manifold of an air compressor, discharging into a volume tank, can be treated as well as the manifold of a combustion engine discharging into the atmosphere.

The exciter piston was mounted on an electrodynamic shaker and is free to move in one of the discharge plenums. The other discharge opening was blocked by a metal plate. All measurements were made with zero mean flow. The presence of mean flow alters the impedances somewhat, but for the low flow velocities typical of this type of compressor it was judged not to be necessary to introduce mean flow. While the methods presented are in principle applicable to mean flow also, the practical difficulty of introducing mean flow at the input location without disturbing the excitation piston or without adding impedances to the manifold that cannot be corrected for, have to be worked out from case to case.

Three quarter-inch microphones were flush mounted at No. 1, 2 and a (Figure 8). The aim was to measure the following:

(1) Z_{11}: input impedance, at the piston, No. 1;
(2) Z_{21}: transfer impedance, at the discharge plenum No. 2 (the input was at the other cylinder's discharge plenum, No. 1);
(3) Z_{a1}: transfer impedance, at the anechoic termination (the input was at the discharge plenum, No. 1).

In dimensionless forms, these impedances are

$$Z_{11}(\omega) = (S_1/\rho c)p_1(\omega)/\dot{X}_1(\omega), \tag{31}$$

$$Z_{21}(\omega) = (S_2/\rho c)p_2(\omega)/\dot{X}_1(\omega), \tag{32}$$

$$Z_{a1}(\omega) = (S_a/\rho c)p_a(\omega)/\dot{X}_1(\omega). \tag{33}$$

The results are presented in the form of impedance level (ZL) and phase (ψ_Z), where impedance level is defined as

$$ZL = 20\log_{10}|\bar{Z}| = 20\log_{10}|Z/(\rho c/S)|(\text{dB}). \tag{34}$$

Note that the impedance level is an absolute quantity. It expresses the dimensionless impedance magnitude $|\bar{Z}|$ in decibels. It could also be interpreted as a relative quantity as

$$ZL = 20\log_{10}(|Z|/Z_{\text{ref}})(\text{dB}), \tag{35}$$

where Z_{ref} is the characteristic acoustic impedance, $Z_{\text{ref}} = \rho c/S$.

Although the ordinates (ZL and ψ_Z) are in dimensionless forms in the plots of results, the abscissa (i.e., the frequency f) is not. This is done because it is difficult to define a reference frequency. The frequencies, here, apply to the air. To make these plots universally applicable, the abscissa has to be converted to either the wave number (k) or the wave length (λ). Both of these account for the medium's speed of sound. Thus, the frequencies for the air can be converted as follows:

$$f \text{ to } k\text{: } 1 \text{ Hz} \rightarrow 4{\cdot}599 \times 10^{-4} \text{ in}^{-1}; \qquad f \text{ to } \lambda\text{: } 1 \text{ Hz} \rightarrow 13\,662 \text{ in.}$$

For example, the speed of sound of refrigerant R-12 at normal compressor discharge conditions is roughly half that of air. Thus the impedance value at 100 Hz for air is applicable to R-12 at 50 Hz. The impedance values from the air test results at frequencies f_{air} are equal to the impedances in the medium, for instance R-12, at frequency f_{m}, where

$$f_m = f_{\text{air}}\, c_m/c_{\text{air}}, \tag{36}$$

where the subscript m refers to the medium.

Before proceeding to the measurement results, it is vital to grasp the dynamic nature of the manifold. An approximate analysis of the inner cavities (consisting of discharge plenums, connecting passages and collector) reveals that there are two important resonant frequencies of gas oscillations: (i) sloshing mode frequency, 390 Hz; (ii) compressive mode frequency, 585 Hz.

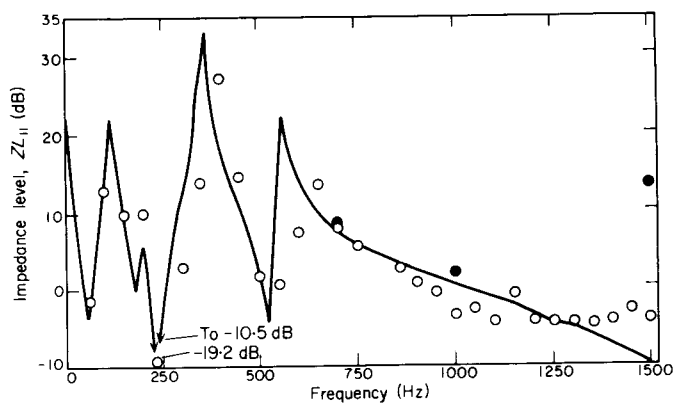

Figure 9. Input impedance level ZL_{11} with harmonic method. o, Experiment (harmonic); ●, experiment (standing wave rule method); ——, Theory.

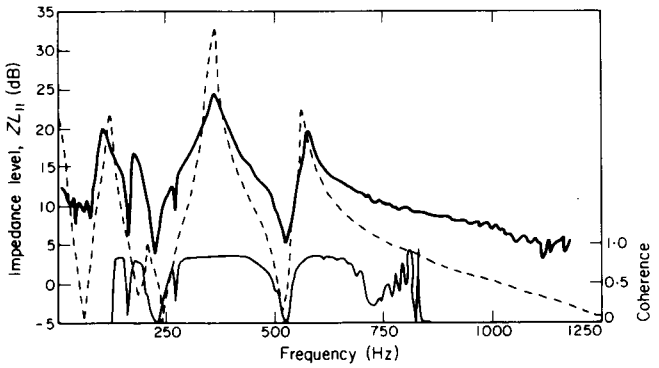

Figure 10. Input impedance level ZL_{22} with random method. ——, Experiment (random); – – –, theory.

Now the question arises: what about the exit piping and muffling system? If the components belonging to one of the cylinders are deleted, then the system is reduced to a single cylinder manifold. It now consists of a discharge plenum, connecting passage, half of the collector and the muffling system. An approximate analysis demonstrated that there are essentially two dominant low frequency resonances, one at 140 Hz and the other is 200 Hz. These are due to the gas oscillations in the components through which mean flow from one compressor would pass. The 390 Hz and 585 Hz resonances are due to the dynamic interactions between cylinders. Thus, if the interference mechanism between cylinders is not accounted for in theoretical computations, only the 120 Hz and 140 Hz resonances would be predicted. (A detailed discussion of the multicylinder manifold modeling along with the procedures for theoretical computations will be the subject of a future paper.)

The measurement results are presented for all three proposed methods. The input impedance magnitude measured by each of the three methods is shown in Figures 9, 10 and 11

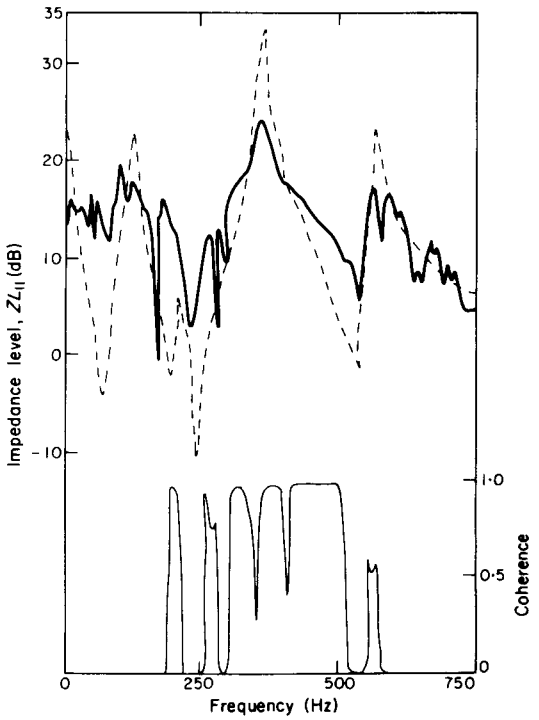

Figure 11. Input impedance level ZL_{11} with transient method. ——, Experiment (transient); – – –, theory.

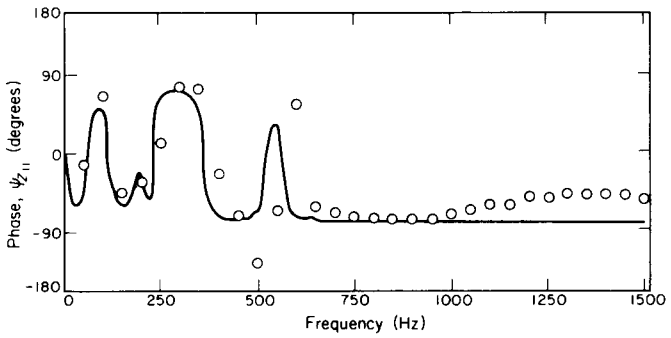

Figure 12. Input impedance phase $\psi_{Z_{11}}$ with harmonic method. o, Experiment (harmonic); ——, theory.

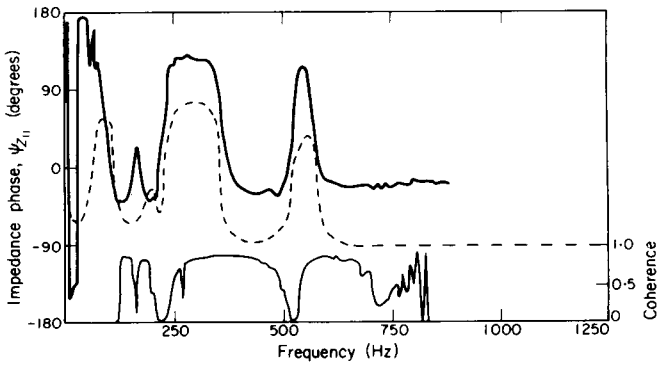

Figure 13. Input impedance phase $\psi_{Z_{11}}$ with random method. ——, Experiment (random); – – –, theory.

as a function of excitation frequency. For a bench mark, and for interpretation, theoretically obtained results are superimposed. Note that the coherence values for the transient and random methods are also given, which made it not practical to superimpose all results in one figure.

Phase information for the input impedance is given in Figures 12, 13 and 14. Again, theoretical results serve as a bench mark.

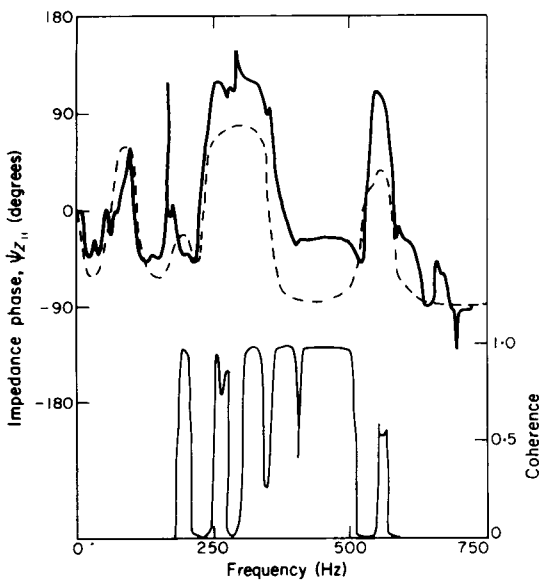

Figure 14. Input impedance phase $\psi_{Z_{11}}$ with transient method. ——, Experiment (transient); – – –, theory.

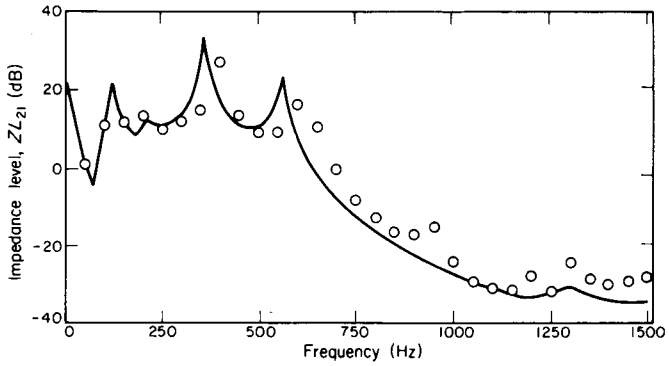

Figure 15. Transfer impedance level ZL_{21} with harmonic method. Legend as Figure 12.

Measured transfer impedance magnitudes and phase angles are given in Figures 15 through 19. Again, theoretical values serve as comparison bench marks and the coherence values for the transient and random excitation methods are given.

The impedance spectra clearly show resonances. The values of the resonant frequencies, as calculated from the approximate analysis, match very well with the experimental results. The resonance at 200 Hz is not dominant at all, but it is noticeable. The resonance at about 140 Hz is pronounced and is more or less of the same order as the compressive mode resonance. The sloshing mode resonance is the most dominant.

The input impedance magnitude ZL_{11} peaks high at the resonances and falls down at antiresonances. Above the compressive mode frequency, the impedance drops gradually and takes on small values in the frequency range of interest. The transfer impedance at point 2, ZL_{21}, shows all the trends of the input impedance except that there are no pronounced antiresonances. In between the resonances, the curve is smooth.

The impedance phase plots reveal that the phase is generally near $-90°$ in the off-resonance regions. Since the resistance is the real part of the impedance, this implies that the resistive component is negligible. The reactive component, the imaginary part of the impedance, is

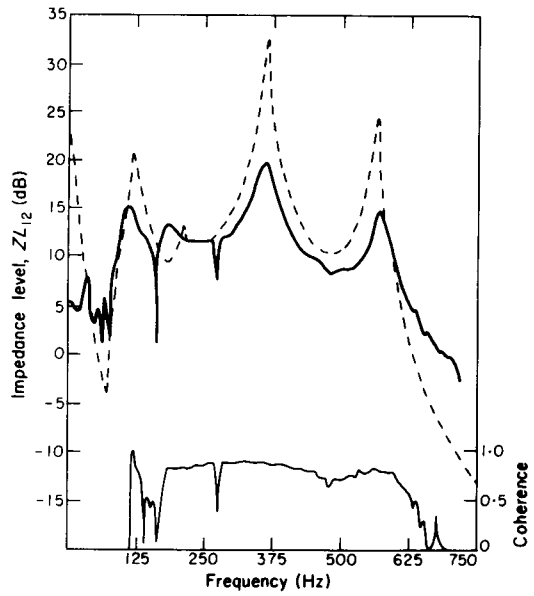

Figure 16. Transfer impedance level ZL_{21} with random method. Legend as Figure 13.

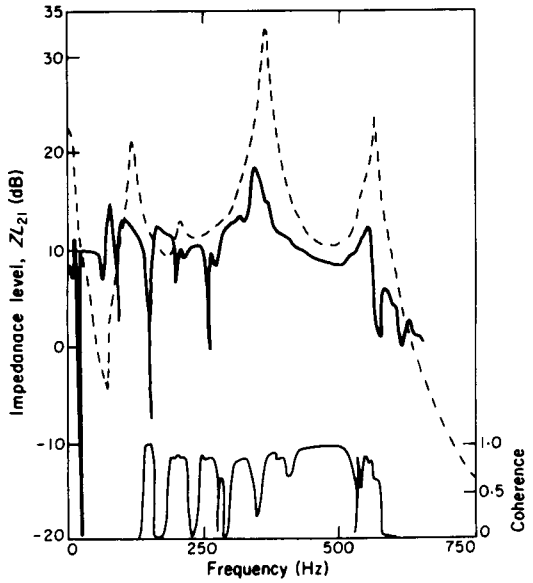

Figure 17. Transfer impedance level ZL_{21} with transient method. Legend as Figure 14.

negative. It is expected to be such because, at low frequencies, elastic properties dictate the system response. In the regions of resonance, the phase is high and takes on positive values. The phase plots show peaks at the resonances. Whereas the input impedance has two distinct peaks at the sloshing and compressible resonances, the plenum transfer impedance $\psi_{Z_{12}}$ peak combines both of these. Again, the anechoic transfer impedance phase plot does not show any contribution from the sloshing resonance.

The measured phase values show good agreement as far as tendency of behavior is concerned. The difference in the measured phase magnitudes between the three types of excitation is caused by the instrumentation response limitations, to which the transient and random methods are most susceptible. The harmonic excitation method is by its nature the most accurate method, since it is less demanding in terms of analysis equipment complexity. The phase disagreement should not be judged to be severe, however, since one has to remember that good phase measurements are difficult to achieve in general.

The measured magnitude values agree with each other fairly well both in magnitude and in tendency. Again, the harmonic method should be the more accurate, against which the transient and random results should be judged.

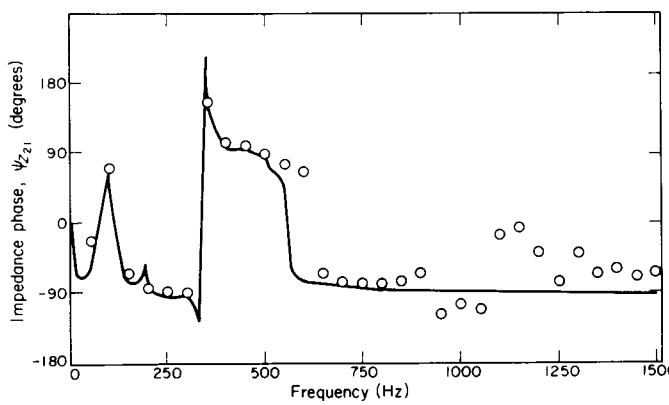

Figure 18. Transfer impedance phase $\psi_{Z_{21}}$ with harmonic method. Legend as Figure 12.

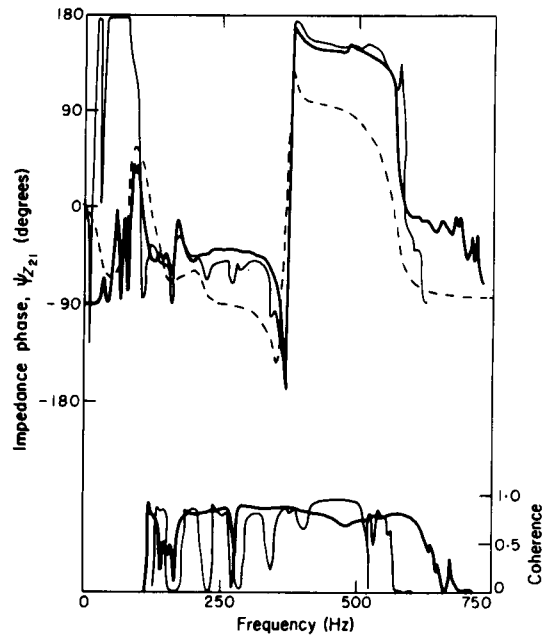

Figure 19. Transfer impedance phase $\psi_{Z_{21}}$ with random and transient methods. ——, Experiment (random); ——, experiment (transient); ---, theory.

6. DISCUSSION

Ambient noise affects the precise measurement of the acoustic impedance. The "ambient noise" term here refers to the sound pressure level present in the acoustic system, in the absence of any excitation. Figure 20 shows the actual and the calculation paths. $p(t)$ is the measured pressure and it includes contributions from both excitation and ambient. At certain frequencies, i.e., at the antiresonances, very low sound pressure levels are obtained. Hence, the measured pressure is predominantly ambient noise level. This is evident from Figure 21, where the transfer impedance magnitude ZL_{a1} is compared for the harmonic and random excitation methods. For the results shown in Figure 21, no spectral averaging was attempted. To unearth the pressure signal from the noise, spectral averaging [13, 14] was utilized. The spectral averaging was done for only the random and transient methods, and not for the harmonic method as the signal to noise ratio was considered to be good at all points except at the anechoic termination. Figures 21 and 22 demonstrate the effect of averaging on the transfer impedance ZL_{a1}. With averaging, all the trends of the system

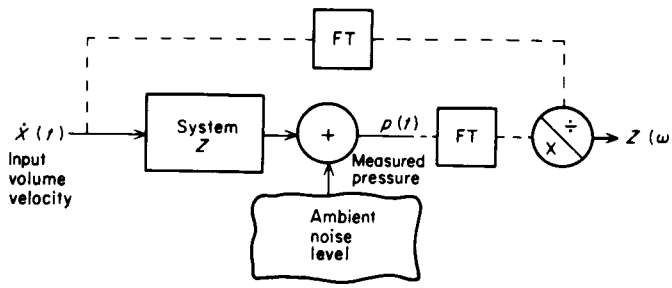

Figure 20. Effect of ambient noise on impedance measurements. ----, Calculation path; ——, actual process path.

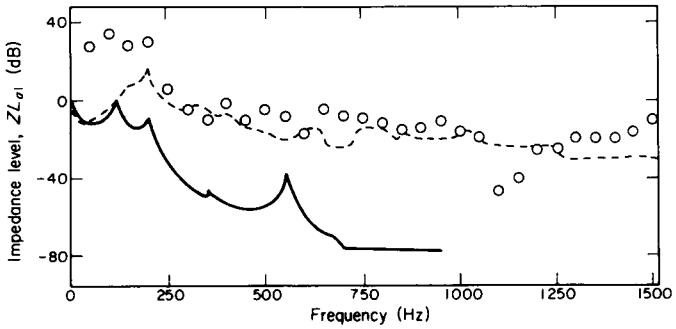

Figure 21. Transfer impedance level ZL_{a1} with harmonic and random methods. o, Experiment (harmonic, without averaging); ---, experiment (random, without averaging); ——, theory.

response are visible but magnitudes are still off. This is due to the dynamic range problem, to be discussed next.

Accuracy of a transfer function measurement depends upon the nature and level (i.e., the energy density form) of the input excitation. Broch [17] has demonstrated this for structural dynamic systems by comparing the frequency sweep method, the impulse response transformation method and the wide band random noise methods.

Transient and random methods suffer from loss in measurement dynamic range. To obtain reliable statistical accurate results, relatively long measurement times are required. For the present application, 100 cycles of averaging was carried out. In spite of the averaging, the dynamic range obtained with transient and random methods is considerably smaller than with the harmonic method.

The harmonic method is the most accurate of all because it is less reliant on good instrumentation response and functioning than the transient and random methods. Although the

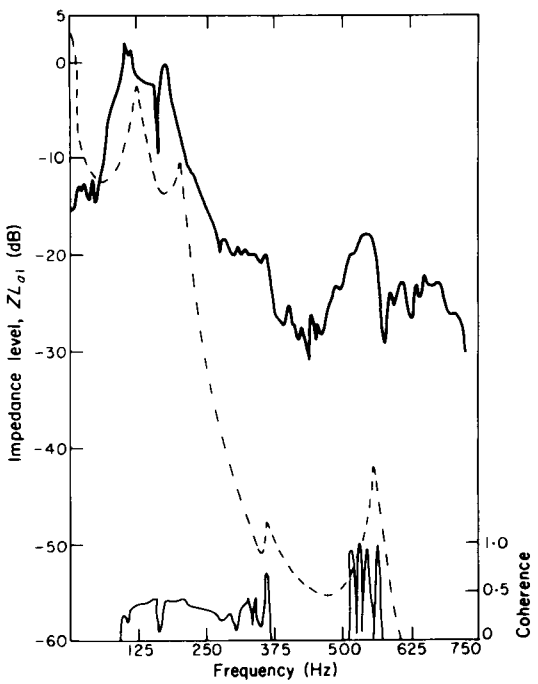

Figure 22. Transfer impedance level ZL_{a1} with random method and spectral averaging. ——, Experiment (random); ---, theory.

method is faster than the conventional impedance measuring methods, it still provides impedances at discrete frequencies only. A large number of frequency points are required to complete the spectra.

Both random and transient methods are certainly much faster, but less accurate, than the harmonic method. The whole spectrum can be obtained with only one measurement. The coherence function shows that the input and output are generally coherent in the region of resonance and incoherent over the rest of the frequency range. Although the impedance levels are not exactly the same as the ones measured by the harmonic method, they follow the trends very well and show all the tendencies. The random and transient measurement procedures provide impedance spectra within the dynamic range of the instrumentation and excitation.

TABLE 1

Comparison of measurement excitations

	Harmonic excitation	Random excitation	Transient excitation
Single frequency measurement	Yes	No	No
Continuous frequency measurement	No	Yes	Yes
Dynamic range	Good	Reduced	Reduced
Way of improvement	Sinusoidal sweep for continuous frequency measurement	Long measurement time required for better dynamic range	Proper choice of excitation function and averaging required for better dynamic range

These methods are compared in Table 1. To obtain better dynamic range, improvements are also suggested and tabulated. Based on Table 1, the following procedure can be recommended for the impedance measurements.

1. Use the random or transient method to obtain the complete impedance spectra. A coherence function analysis will separate the useful part from the spurious part. Establish the critical region in the spectra.
2. Take enough data, by the harmonic method, to establish the true magnitudes.

Thus, in brief, the harmonic and random or transient methods are complementary to each other.

Some of the measurement inadequacies and sources of error are as follows.

(i) The maximum particle displacement is limited by the fact that the shaker has a constant acceleration. Thus, with increasing frequencies, the displacement becomes smaller and smaller. It has to be substantially higher than the transducer noise.
(ii) The displacement transducer calibration could be done only above 0·001 inch. The calibration was extrapolated for the lower displacements.
(iii) The microphone accuracy is, at the most, $\pm 0{\cdot}5$ dB.
(iv) Errors can arise from magnitude and phase distortion in the instrumentation.

Note that measured impedance magnitude and phase differences between the three methods are mainly due to instrumentation response limitations and this does not imply that there is anything wrong with using an oscillating piston as the volume source.

7. CONCLUDING REMARKS

An acoustical impedance measurement technique has been presented. It is oriented towards the determination of the system-dynamic characteristics of the manifolds of positive displacement fluid machinery. The investigation is geared towards the lower frequencies as these influence the machinery performance.

A harmonically oscillating piston is used as the driver. A digital Fourier analyzer is used for the data acquisition and processing. The impedances are computed from the measurement of input volume velocity and manifold acoustic pressure response. Both input and transfer impedances can be measured efficiently and directly. Harmonic, random and transient excitations are used. Although the harmonic excitation provides only point by point impedances, the dynamic range is excellent. With the random and transient excitations the measurement dynamic range is reduced but continuous impedance measurement is provided. The technique has been applied to a two-cylinder compressor discharge system. The validity of the method has been demonstrated by comparing results with theory.

The concept of measuring impedances in this fashion has perhaps existed for a long time but the advent of digital processing hardware and the availability of the Fast Fourier Transform routines has now made it possible. Recently it has been applied to structural dynamic systems [18]. The acoustical systems, however, are non-dispersive and have travelling wave solutions. Unlike the situation for structural systems, only one variable (i.e., acoustical pressure) can be measured reliably, in general, in the plane wave region. Perhaps the technique presented here resembles the force gauge and accelerometer equipped impedance head method now used for the evaluation of structural vibrations.

The shortcomings of the equipment described are as follows. The technique presented here is directly applicable to the study of the dynamic characteristics of manifolds. However, it needs to be modified for the evaluation of the acoustical performance of individual elements and mufflers. Furthermore, the experiment did not include any mean fluid flow effects. In the technique steady-state excitations are employed, except in the case of the transient excitation where it is of a pseudo-steady-state type. This excitation could have been improved to obtain better power spectral density and thus more dynamic range. This experiment might have been improved by using feedback resonance control methods as they are available and have been used for structural dynamic systems [18].

ACKNOWLEDGMENTS

The authors wish to express their gratitude to Carlyle Compressor Company, Carrier Corporation for sponsoring the project. Special thanks are due to P. K. Baade of Carrier Research Division.

REFERENCES

1. R. SINGH, E. SANDGREN, K. RAGSDELL and W. SOEDEL 1976 *ASME Winter Annual Meeting, Special Session, Computer Design of Fluid Machinery*. Simulation of a two cylinder compressor for discharge gas pressure oscillation prediction.
2. R. SINGH and W. SOEDEL 1976 *Proceedings of Purdue Compressor Technology Conference, West Lafayette, Indiana, U.S.A.*, 271–281. Fluid dynamic effects in the multicylinder compressor suction and discharge cavities.
3. W. S. GATLEY and R. COHEN 1969 *Journal of the Acoustical Society of America* **46**, 6–16. Methods for evaluating the performance of small acoustic filters.
4. W. S. GATLEY 1967 *Ph.D. Thesis, Purdue University*. Development and evaluation of methods for design of mufflers in small refrigeration systems.
5. L. L. BERANEK 1949 *Acoustic Measurements*. New York: John Wiley.

6. American Society of Testing Materials 1972 *ASTM C*384-58. Impedance and absorption of acoustical materials by the tube method.
7. R. J. ALFREDSON and P. O. A. L. DAVIES 1971 *Journal of Sound and Vibration* **15**, 175–196. Performance of exhaust silencer components.
8. T. H. MELLING 1973 *Journal of Sound and Vibration* **28**, 23–54. An Impedance tube for precision measurement of acoustic impedance and insertion loss at high sound pressure levels.
9. K. U. INGARD and V. K. SINGHAL 1973 *Journal of the Acoustical Society of America* **54**, 1343–1346. Upstream and downstream sound radiation into a moving fluid.
10. J. IGARASHI and M. TOYAMA 1958 *University of Tokyo, Aeronautical Research Institute, Report* 339, 24(10). Fundamentals of acoustic silencers (I). Theory and experiment of acoustic low pass filters.
11. T. MIWA and J. IGARASHI, 1959 *University of Tokyo, Aeronautical Research Institute, Report* 344, 25(4). Fundamentals of acoustic silencers (II). Determination of four terminal constants of acoustic elements.
12. T. SALARA 1974 *Journal of the Audio Engineering Society* **22**, 146–153. Sources of constant volume velocity and their use for acoustic measurements.
13. J. S. BENDAT and A. G. PIERSOL 1971 *Random Data: Analysis and Measurement Procedures.* New York: John Wiley.
14. P. R. ROTH 1971 *IEEE Spectrum* **4**, 62–70. Effective measurements using digital signal analysis.
15. S. N. RSCHEVKIN 1963 *Course of Lectures on the Theory of Sound.* New York: MacMillan Company.
16. P. M. MORSE and K. U. INGARD 1968 *Theoretical Acoustics.* New York: McGraw-Hill Book Company.
17. J. T. BROCH 1975 *B & K Technical Review* **4**, 3–41. On the measurement of frequency response functions.
18. P. CHAPMAN, 1975 *Shock and Vibration Information Center, Naval Research Laboratory, Washington, D.C., Seminar on Understanding Digital Control and Analysis in Vibration Test Systems* **1**, 1–71. Digital vibration control techniques.

APPENDIX: NOMENCLATURE

c speed of sound (m/s)
f frequency (Hz)
FT Fourier Transform
G power spectral density (dB)
j $\sqrt{-1}$
k wave number (m^{-1})
l length (m)
p acoustic pressure (N/m^2)
S cross-sectional area (m^2)
t time (s)
x acoustic particle displacement (m)
X acoustic volume displacement (m^3)
$\dot{X}$ acoustic volume velocity (m^3/s)
Z acoustic impedance (N-s/m^5)
$\bar{Z}$ dimensionless impedance
ZL impedance level (dB)
λ wavelength (m)
ρ mean fluid density [N-s^2/m^4]
ψ phase of a complex quantity
ω circular frequency (rad/s)

Subscripts

1 driving point, input excitation chamber
2 cross-point in other chamber
a cross-point at anechoic termination
e excitation frequency
I imaginary part
R real part